ELECTRONICS AND ELECTRICAL ENGINEERING
ISSN 1392 – 1215 *2010. No. 3(99)*
ELEKTRONIKA IR ELEKTROTECHNIKA

ELECTRICAL ENGINEERING
T 190
ELEKTROS INŽINERIJA

Magnetic Field of Inductive Loop – Theory and Experimental Results

P. Spalevic, B. Miric
Faculty of Technical Science, State University of Novi Pazar,
Vuka Karadžića bb,36300, Novi Pazar, Serbia, tel.: +38120/317-752, e-mail: petarspalevic@yahoo.com, bmiric@np.ac.rs
D. Vuckovic
Faculty of Technical Science, University of Pristina,
Kneza Milosa 7, 38220 Kosovska Mitrovica, Serbia, tel.: +38128425320, e-mail: darkovuckovic@yahoo.com
S. Panic
Faculty of Electronic Engineering, University of Nis, Aleksandra Medvedeva 14, 18000 Nis, Serbia,
tel.: +38163470649, e-mail: stefanpnc@yahoo.com

Introduction

Constructively, the inductive loops are realized by pairing of well conductive metal bands on the roadway or by introducing coils with inductive loop in the prepared fissures in the roadway [1-2]. They are supplied from some high frequency generator whose frequency is between 20 KHz and 200 KHz. Vehicle whose velocity is measured generates one brief signal in inductive loop (the change in current, namely voltage in inductivity of the loop that is the part of the oscillatory circuit adjusted on the frequency generator) [3]. The impulse can be comprehended as a consequence of electromagnetic influences of conductive, metal parts of vehicle on loop.

In the electrical view, vehicle can be described as one equivalent conductive surface that is located approximately on the bottom of vehicle. for skin-effect influences, only the bottom of vehicle have the effective influence on the inductive loop [4-5]. On the 100 kHz frequency the depth of action of high frequency field is about 0.04 mm. As descripted conductive equivalent surface approaches, that moves in the direction of vehicle vector practically parallel with roadway and also with inductive loop, that surface acts more and more like an short circuited coil [6]. Vertical movements of vehicle that exist as consequence of road roughness are neglected [7]. Coupling between inductive loop and the equivalent surface increases as equivalent surface approaches to inductive loop[8].

Magnetic field of rectangular loop

Next example is magnetic field around rectangular loop shown on Fig. 1.

Vector of the magnetic induction in point M will be:

$$\begin{cases} \vec{B}_M = \vec{B}_1 + \vec{B}_2 + \vec{B}_3 + \vec{B}_4 = \left(\vec{B}_{1x} + \vec{B}_{2x} + \vec{B}_{3x} + \vec{B}_{4x}\right)\hat{x} + \\ + \left(\vec{B}_{1y} + \vec{B}_{2y} + \vec{B}_{3y} + \vec{B}_{4y}\right)\hat{y} + \left(\vec{B}_{1z} + \vec{B}_{2z} + \vec{B}_{3z} + \vec{B}_{4z}\right)\hat{z} \\ \vec{B}_M = \vec{B}_x\,\vec{x} + \vec{B}_y\,\vec{y} + \vec{B}_z\,\vec{z}, \quad B_M = \sqrt{B_x{}^2 + B_y{}^2 + B_z{}^2} \end{cases} . \tag{1}$$

If we accept orientation of Decart coordinate system like on Fig.1 than three components of vector will be:

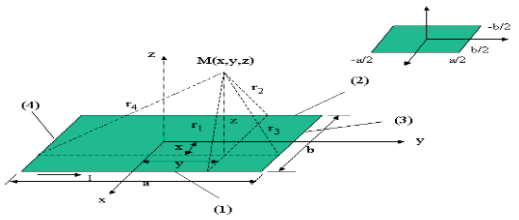

Fig. 1. Magnetic field around rectangular loop

$$B_x(x,y,z) = \frac{\mu_0 I}{4\pi}\left(\frac{\frac{y}{a_1}b_1 - \frac{y}{a_2}b_2}{b_1 b_2} - \frac{\frac{y}{a_3}b_3 - \frac{y}{a_4}b_4}{b_2 b_1}\right), \tag{2}$$

$$B_y(x,y,z) = \frac{\mu_0 I}{4\pi}\left(\frac{\frac{z+z_0}{a_3}b_5 - \frac{z+z_0}{a_1}b_6}{b_5 b_6} - \frac{\frac{z-z_0}{a_4}b_7 - \frac{z-z_0}{a_2}b_8}{b_8 b_7} - \right.$$
$$\left. - \frac{\frac{x+x_0}{a_1}b_1 - \frac{x+x_0}{a_2}b_2}{b_1 b_2} - \frac{\frac{x-x_0}{a_3}b_3 - \frac{x-x_0}{a_4}b_4}{b_3 b_4}\right), \tag{3}$$

$$B_z(x,y,z) = \frac{\mu_0 I}{4\pi}\left(\frac{\frac{y}{a_4}b_7 - \frac{y}{a_2}b_8}{b_7 b_8} - \frac{\frac{y}{a_3}b_5 - \frac{y}{a_1}b_6}{b_5 b_6}\right), \tag{4}$$

where x, y, z – coordinates of the point M; x_0, z_0 – dimensions of the loop.

$$\begin{cases} a_1 = \sqrt{(x-x_0)^2 + y^2 + (z+z_0)^2}, \\ a_2 = \sqrt{(x+x_0)^2 + y^2 + (z-z_0)^2}, \\ a_1 = \sqrt{(x+x_0)^2 + y^2 + (z+z_0)^2}, \\ a_1 = \sqrt{(x-x_0)^2 + y^2 + (z-z_0)^2}, \\ b_1 = z - z_0 + a_2, \qquad b_2 = z + z_0 + a_1, \\ b_3 = z - z_0 + a_4, \qquad b_4 = z + z_0 + a_3, \\ b_5 = x - x_0 + a_1, \qquad b_6 = x + x_0 + a_3, \\ b_7 = x - x_0 + a_2, \qquad b_8 = x + x_0 + a_4. \end{cases} \quad (5)$$

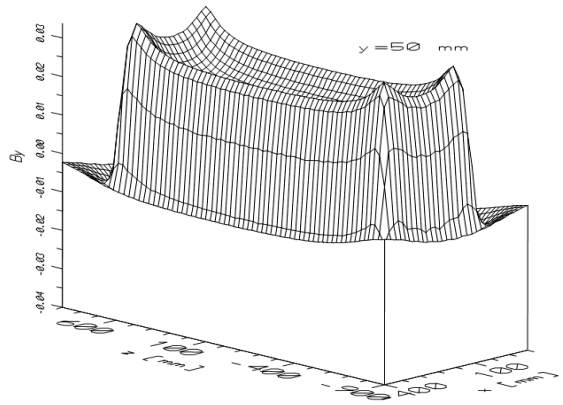

Fig. 2a. Component Bx for rectangular loop (dimensions 1500 x 500 mm), 50 mm above the loop.

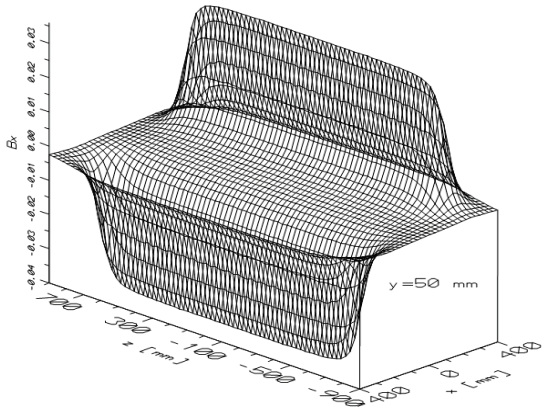

Fig. 2b. Component By for rectangular loop (dimensions 1500 x 500 mm), 50 mm above the loop

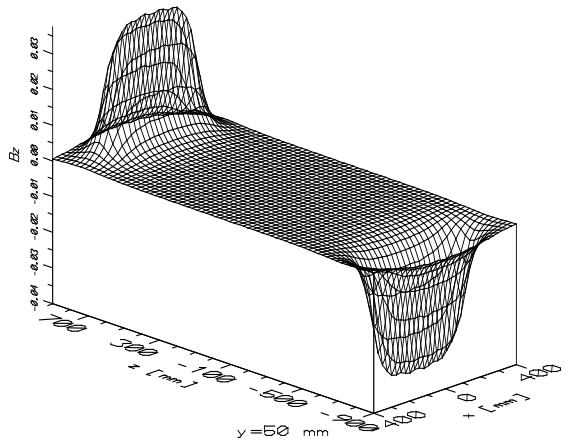

Fig. 2c. Component Bx for rectangular loop inductivity (dimensions 1500 x 500 mm), 50 mm above for rectangular loop

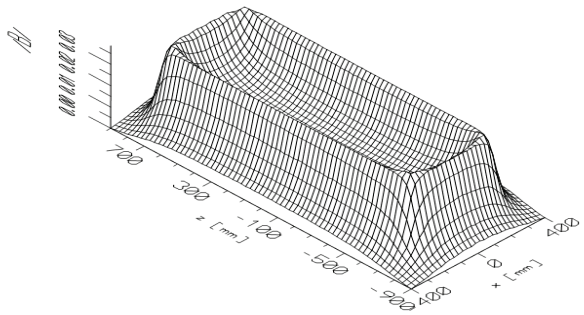

Fig. 2d. Intensity of vector magnetic inductivity rectangular loop (dimensions 1500 x 500 mm),50 mm above the loop

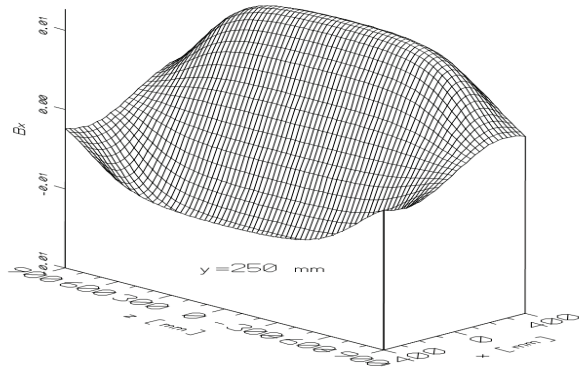

Fig. 3a. Component Bx for rectangular loop (dimensions1500 x 500 mm), 250 mm above the loop

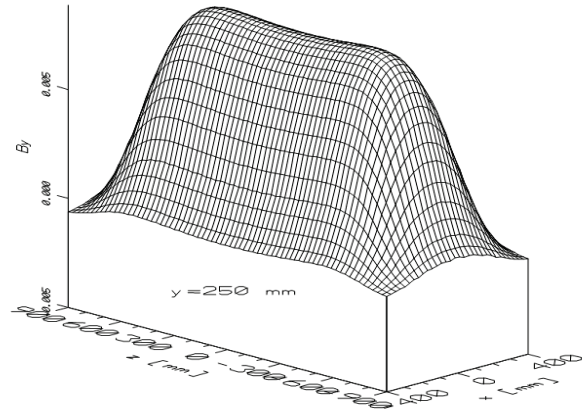

Fig. 3b. Component By for rectangular loop (dimensions 1500 x 500 mm), 250 mm above the loop

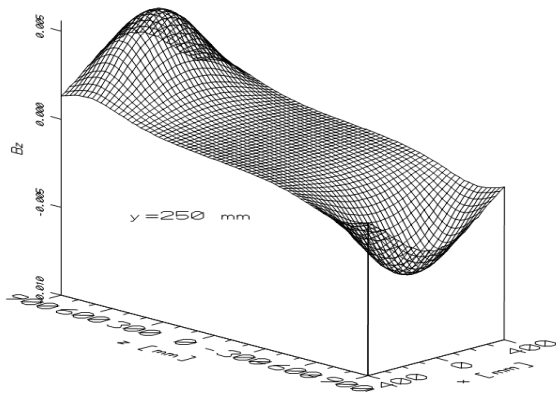

Fig. 3c. Component Bx for rectangular loop (dimensions 1500 x 500 mm), 250 above the loop

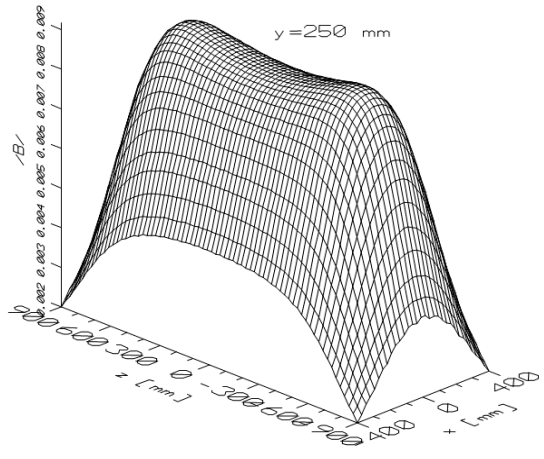

Fig. 3d. Intensity of vector magnetic inductivity for rectangular loop (dimensions 1500 x 500 mm), 250 mm above the loop

We shall now consider case shown on Fig.4 and 5 One loop (in first approximation - bottom of vehicle) is moving above second induction loop. Position of vehicle is determined by vehicle offset Δx. Dimensions of vehicle is 4 x 1.6 m and dimensions of the induction loop is 1.5 x 1.5 m.

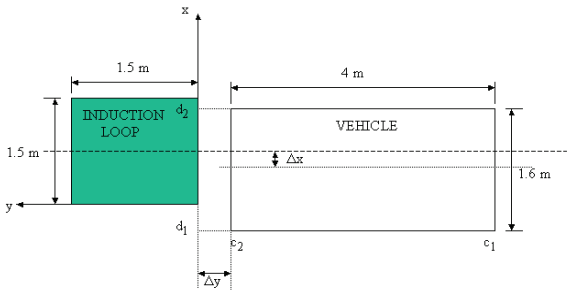

Fig. 4. Dimensions of the vehicle and loop

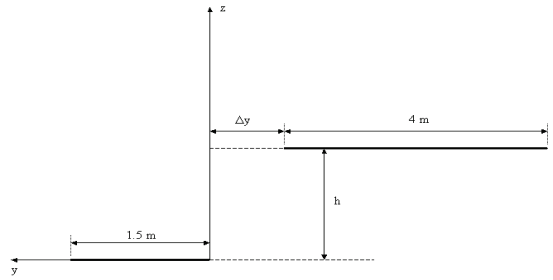

Fig. 5. Distance between the vehicle bottom and loop is h

The most interesting case is when the vertical distance between loops is h=25 cm. Bottom of the most PKV vehicles has that distance from the loop. So, on next figure is shown induction coefficient M in function of vehicle position Δy for different vehicle offset Δx and for h=25 cm (Fig. 6).

Another interesting case is when the width of the vehicle (loop) is less then the width of induction loop (Fig.7). We have that case when vehicle is motorcycle or other small vehicle. On Fig.7 length of the induction loop is changed from 1.5 to 0.5 meters (Fig. 7).

On next figures are shown induction coefficient M in function of vehicle offset □x and position of vehicle above induction loop □y, for different vertical distance between the loops h (Fig. 8).

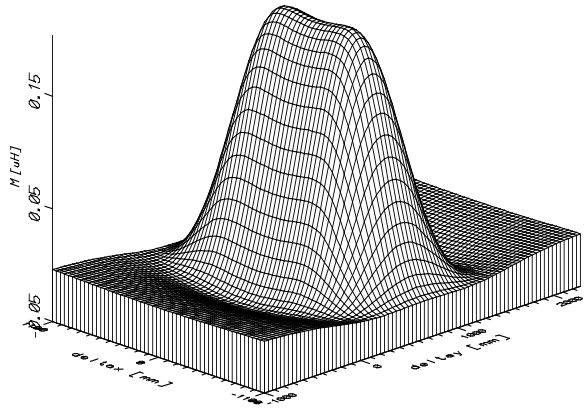

Fig. 6. Induction coefficient M in function of vehicle position Dy for different values of vehicle offset Δx and h=25 cm

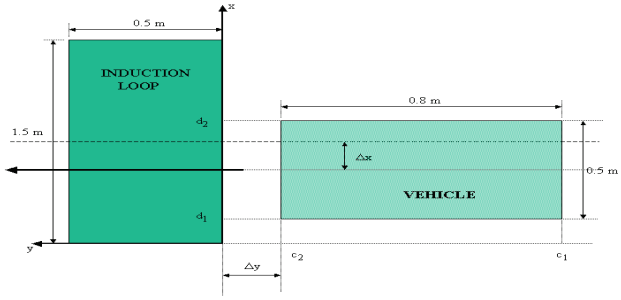

Fig. 7. Width of the vehicle is less than induction loop

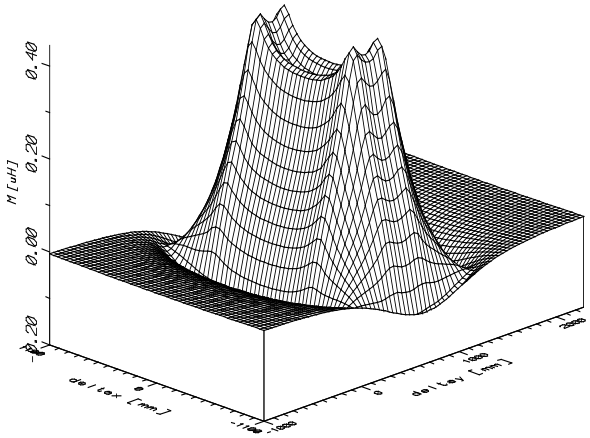

Fig. 8. Induction coefficient M in function of vehicle offset Δx and position of vehicle above induction loop Δy for h=5cm

At last we tried to determine experimentally changing of induction coefficient M in function of vehicle position Δy. As vehicle loop we used metal plate with dimensions 500 x 800 mm (Fig.7). Induction loop was connected to the equipment ESOMAT 2000. Metal plate was 5 cm above the induction loop. In each position of metal plate we the pulse width was measured in phase detector that is in equipment ESOMAT 2000. When vehicle is moving above the loop, it modulated width and phase of pulses.

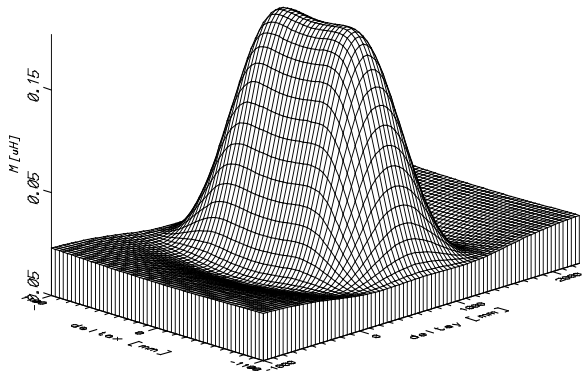

Fig. 9. Induction coefficient M in function of vehicle offset Δx and position of vehicle above induction loop Δy for h=25 cm

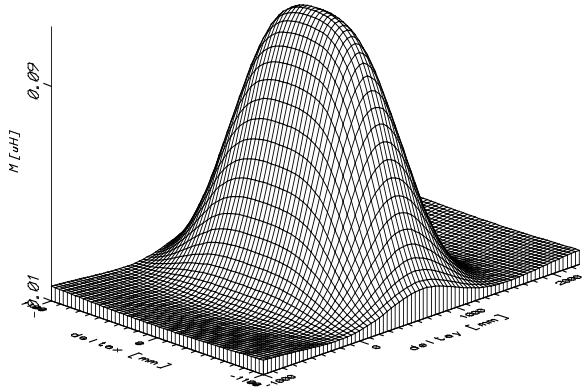

Fig. 10. Induction coefficient M in function of vehicle offset Δx and position of vehicle above induction loop Δy for h=45 cm

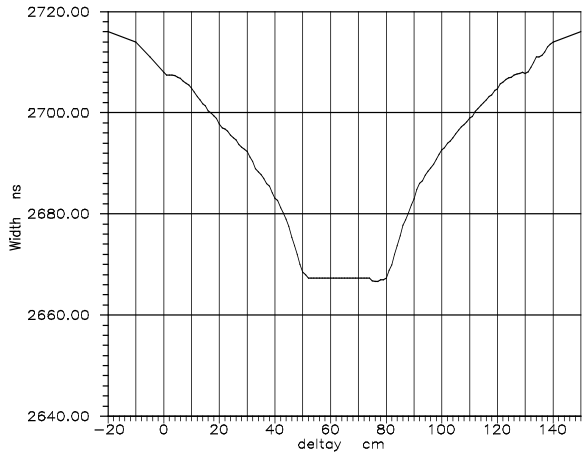

Fig. 11. Pulse width in ns as a function of metal plate position Δy when metal plate offset was Δx=0

On Fig. 11 shown width of pulses in ns as a function of metal plate position D_y when metal plate offset was Δx =0. The same is on Fig.12 but with metal plate offset Δx =50 cm.

Then we used metal carriage and three inductive loops with different dimensions, inductivity and working frequency (Fig.13).

The metal carriage moving above the loops more times, each time with different offset Δx. The amplitude of pulses were measured in equipment ESOMAT 2000 for each value of offset Δx. On Fig. 14 is shown pulse amplitude as a function of metal carriage offset Δx.

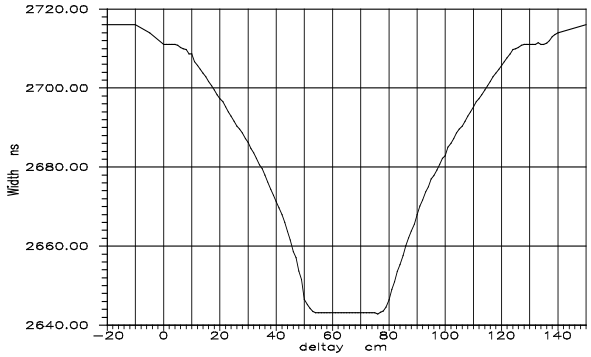

Fig. 12. Pulse width in ns as a function of metal plate position Δy when metal plate offset was Δx=50 cm

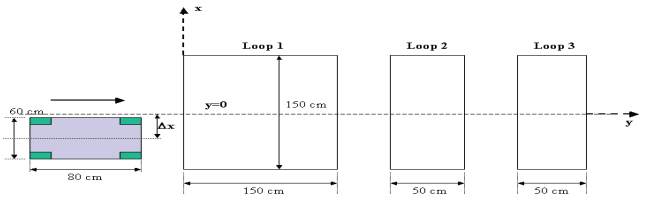

Fig. 13. Metal carriage moving above the three different loop

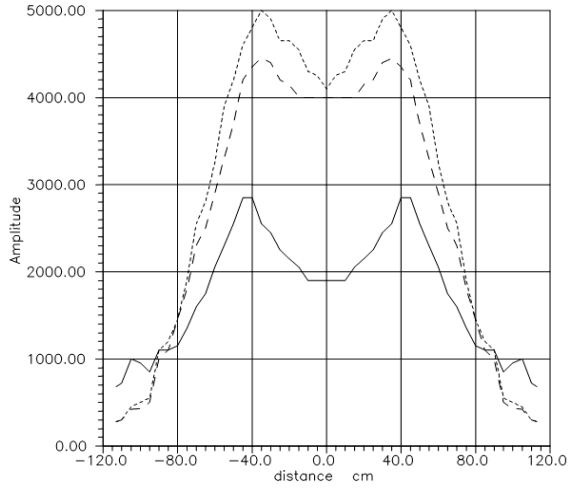

Fig. 14. Pulse amplitude as a function of metal carriage offset Δx

Experimental results

The induction loop were placed on the road inside Physikalisch Techniche Bundesanstalt-PTB near Bessel bau Fig. 15 and 16. The figures shows the position of induction loop used equipment and marks on the road.

Dimensions of the loop and its connection to the measuring equipment that were placed in PTB laboratory is shown on Fig. 16.

This measurement was performed under the known conditions (type of vehicle, position against the loop). The vehicle was OPEL Omega-A and it passed-through over the loops 46 times with different velocities and path but without acceleration. With this second measurement (with video camera) we tried to locate the moment (position of vehicle above the loop) when camera is triggered by

equipment TRAFFIPHOT III fabricated by Traffipax-Vetrieb from Dusseldorf. For this purpose we took corresponding frame from the digitized video camera signal (video camera near Camera A on Fig.17).

Fig. 15. Measuring disposition and equipment

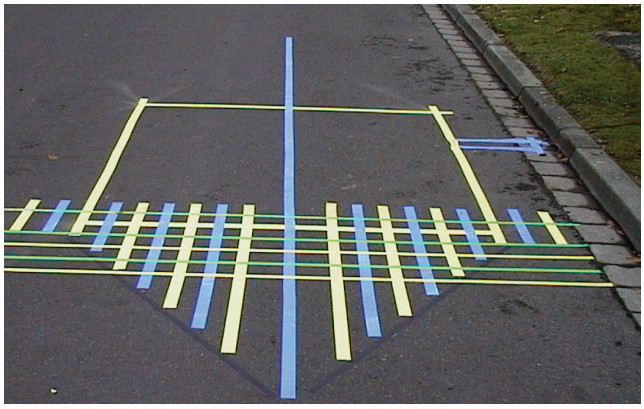

Fig. 16. Induction loop with marks on the road

Camera A was triggered by TRAFFIPHOT III that was connected to the induction loop. Camera B was triggered when front part of vehicle cut the laser beam. Laser beam was 1.11 m from the beginning of the loop. The beam was above the road about 70 cm. Vehicle cut laser beam with its front part where OPEL mark is located.

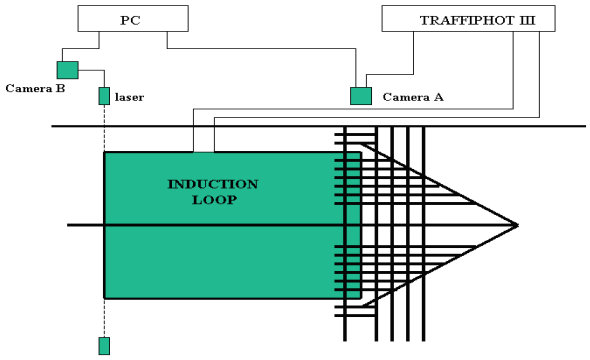

Fig. 17. Sketch of the measuring disposition

The time delay of digital camera is 40 ms but also we must take account the time delay of TRAFFIPHOT equipment. So, whole time delay from the moment when vehicle triggered the TRAFFIPHOT to the moment when camera get a photo is greater than 40 ms. Position of vehicle on a photo is not the position of vehicle when triggering occurs. For different velocities real position of vehicle in that moment differs from the position on photo. The triggering take place ΔS[m] before vehicle position on photo. For Δt=40 ms and vehicle velocity 50 km/h ΔS is 55.5 cm.

On Fig. 18 photos from Camera A are shown. Original digital photo has two half pictures and we separated them with Adobe Photoshop and Adobe Premiere program. Vehicle velocity was measured by laser equipment. On all this photos vehicle velocity was about 20 km/h vehicle offset □x was 0 cm.

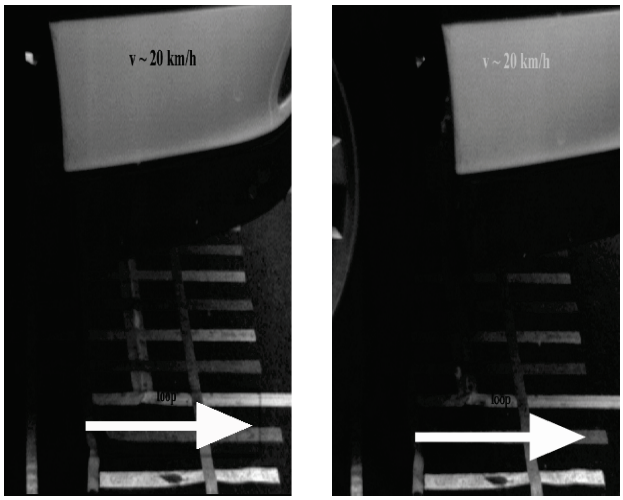

Fig. 18. Photos from camera A. Left photo is first half picture and right photo is second half picture; Δx=0 cm; Δt=253.1 ms; V_a~16.41 km/h

Conclusion

On the basis of conducted measurements and obtained atlas of photographs, it can be concluded that the triggering point of the device connected to the inductive loop depends on the distance between the bottom of the vehicle and the inductive loop. It means that triggering of device connected to the inductive loop will occur later in the case of long vehicle (LKV) than in the case of automobile (PKV). For motorcycle no any triggering was registered during its passage above inductive loop, due to its small surface and negligible value of induction coefficient between the bottom of the motorcycle and inductive loop. Triggering point of the vehicle depends also on the vehicle offset between vehicle and loop axes, in other words on the effective surface covering the inductive loop.

Our measurements indicate that the vehicle distance on which the induction coefficient reaches its critical value when triggering of device occurs, depends above all on the vehicle offset. The vehicle velocity does not influence significantly on the triggering point of connected device.

References

1. **Mirić B., Marković A.** Loop phase detector, part one // Physikalisch-Technische Bundesanstalt, PTB Laborbericht PTB. – September, 1992. – No. 1. – P. 63–95.
2. **Mirić B., Marković A.** Loop phase detector, part two // Physikalisch-Technische Bundesanstalt, PTB Laborbericht PTB. – December, 1992. – No. 1. – P. 63–92.

3. **Mirić B., Vučković D., Spalević P.** Characteristics of Inductive Loops applied in Thelematics // Facta Universitatis, Series: Electronics and Energetics. – April 2006. – No. 1(19). – P. 147–156.
4. **Mirić B.** Inductive loops, theory and measurements // Physikalisch-Technische Bundesanstalt, PTB Laborbericht PTB. – December 1997. – No. 1. – P. 150–170.
5. **Marković A., Kapković J., Luehrs C-H., Michel M., Mirić B., Jaeger, F.** Geschwindigkeitsmessungen im Strassenverkehr // Expert Verlag Stuttgart, SRN Tech. Rep. – May 1996. – P. 292–296.
6. **Mirić B., Kapković J., Marković A.** Merenje brzine vozila u saobračaju na putevima. – Univerzitet u Prištini. – 1995. – 301 p.
7. **Goydke H., Jaeger F., Michel M., Marković A., Mirić B.** Pruefverfahren fuer Geschwindigkeitsmessagerate. – Braunschweig. – December 1992. – P. 160–161.
8. **Jager F., Grottker U., Schrepf H., Guse W.** Prediction signal processing for speed enforcement measuring speed and distance // Computer Standards & Interfaces. – September 2006. – No 1(28). – P. 327–335.

Received 2009 12 03

P. Spalevic, B. Miric, D. Vuckovic, S. Panic. Magnetic Field of Inductive Loop – Theory and Experimental Results // Electronics and Electrical Engineering. – Kaunas: Technologija, 2010. – No. 3(99). – P. 83–88.

Characteristics of inductive loop applied in telematics are presented. First we have theoretically described the distribution of the magnetic field and coupling between the inductive loop and the bottom of vehicle. At last we tried experimentally to confirm obtained results. Ill. 18, bibl. 8 (in English; summaries in English, Russian and Lithuanian).

П. Спалевич, Б. Мирич, Д. Вуцкович, С. Панич. Магнитное поле индуктивной петли – теория и экспериментальные результаты // Электроника и электротехника. – Каунас: Технология, 2010. – № 3(99). – С. 83–88.

Представлены характеристики индуктивных петлей, применяемых в телематике. Сначала теоретически описано распределение магнитного поля и связь между индуктивной петлей и нижней частью транспортного средства. Полученные результаты экспериментально подтверждены. Ил. 18, библ. 8 (на английском языке; рефераты на английском, русском и литовском яз.).

P. Spalevic, B. Miric, D. Vuckovic, S. Panic. Induktyvinės kilpos magnetinis laukas – teorija ir eksperimentiniai rezultatai // Elektronika ir elektrotechnika. – Kaunas: Technologija, 2010. – Nr. 3(99). – P. 83–88.

Pateiktos telematikoje naudojamos induktyvinės kilpos charakteristikos. Pirmiausia teoriškai aprašomas magnetinis laukas ir induktyvinės kilpos bei automobilio dugno tarpusavio sąsajos principai. Pabaigoje eksperimentiškai patikrinami gauti rezultatai. Il. 18, bibl. 8 (anglų kalba; santraukos anglų, rusų ir lietuvių k.).

DOI: 10.5755/j02.eie.9911